

Excellent thermal stability and bulk glass forming ability of Fe-B-Nb-Y soft magnetic metallic glass

著者	Lee Sangmin, Kato Hidemi, Kubota Takeshi, Yubuta Kunio, Makino Akihiro, Inoue Akihisa
journal or publication title	Materials Transactions
volume	49
number	3
page range	506-512
year	2008
URL	http://hdl.handle.net/10097/52321

Excellent Thermal Stability and Bulk Glass Forming Ability of Fe-B-Nb-Y Soft Magnetic Metallic Glass

Sangmin Lee^{1,*1,*2}, Hidemi Kato², Takeshi Kubota², Kunio Yubuta², Akihiro Makino² and Akihisa Inoue³

¹Department of Materials Science, Graduate School of Engineering, Tohoku University, Sendai 980-8579, Japan

²Institute for Materials Research, Tohoku University, Sendai 980-8577, Japan

³Tohoku University, Sendai 980-8577, Japan

Effects of Y addition on the glass forming ability (GFA) of a Fe-B-Nb marginal glass former, and annealing effects on glassy/supercooled liquid phases as well as soft magnetic properties in the multicomponent Fe-B-Nb-Y alloy system were investigated. The origin of highly improved GFA in the multicomponent system is discussed with related to a characteristic exothermic phase transformation, chemical short range ordering, in the supercooled liquid region due to the positive heat of mixing between Nb-Y elements. The separating tendency between Nb and Y elements is considered to suppress precipitation of metastable Fe₂₃B₆ and α -Fe crystalline phases, thus to result in highly improving GFA and distinct high thermal stability against heat treatment of the alloy system. In addition, a glassy ring was fabricated by copper mold casting and magnetic properties were investigated before/after heat treatment. [doi:10.2320/matertrans.MBW200732]

(Received October 30, 2007; Accepted January 11, 2008; Published February 20, 2008)

Keywords: metallic glasses, iron-based alloy, high thermal stability, excellent soft magnetic properties

1. Introduction

More and more attention has been paid to Fe-based bulk metallic glasses (BMGs) due to the high fracture strength, hardness, corrosion resistance¹⁻³ and their excellent soft-magnetic properties. The excellent soft-magnetic Fe-based BMGs are considered to be useful for magnetic field shielding materials, transformer core materials and perpendicular magnetic memory device. A soft-magnetic underlayer, absolutely necessary for the perpendicular magnetic memory device, is required to have high thermal stability enough to sustain the good soft-magnetism during thermal treatments. What is more, the Fe-based BMG is one of the most appropriate candidates for precision devices such for micro-motor and NEMS associated with the nanoimprinting technique, since these have good merits for processing of extremely fine configuration by the Newtonian viscous flow at the supercooled liquid region as well as good soft-magnetic properties, comparing with both conventional crystalline materials and non-ferrous BMGs. In spite of these advantages, low glass forming ability (GFA) and poor thermal stability of the Fe-based BMGs have restricted those industrial applications. Recently, the effects of the rare earth (RE) elements such as Y upon the Fe-based glass formers are reported by DH. Kim *et al.* (Yonsei Univ., Korea).⁴ A lot of scientists in the world are investigating the effectiveness of the rare earth elements addition upon the Fe-based glass formers, and a couple of reports about the high GFA of the Y added Fe-based amorphous alloys have been already published. Nevertheless, the magnetic properties of the Y bearing Fe-based BMGs are not included in the almost reports.⁴⁻¹¹⁾

In this paper, the effects of Y addition on GFA of a Fe-B-Nb marginal glass former, and annealing effects on glassy/supercooled liquid phases and soft magnetic properties in the

multicomponent Fe-Nb-B-Y alloy system were investigated. The origin of highly improved GFA in the multicomponent system is discussed with related to a characteristic exothermic phase transformation, chemical short range ordering, in the supercooled liquid region due to the positive heat of mixing between Nb-Y elements. The separating tendency between Nb-Y is considered to suppress precipitation of metastable Fe₂₃B₆ and α -Fe crystalline phases, thus to result in highly improving GFA and distinct high thermal stability against heat treatment of the alloy system. This tendency is also considered to raise the internal stress frozen in the as-cast BMG, which degrades the soft magnetic properties, *i.e.* coercivity and permeability. However, these soft magnetic properties could be improved by the appropriate heat treatments enabled by the distinct high-thermal stability of this alloy composition.

2. Experimental Procedures

Glassy ribbons and rods of (Fe_{0.72}B_{0.24}Nb_{0.04})_{100-x}Y_x ($x = 0 \sim 6$) were prepared in an argon atmosphere by the single-roller melt spinning technique and copper-mold casting technique, respectively. Firstly, Fe₇₂B₂₄Nb₄ pre-alloy ingots were obtained by induction melting with Fe (99.9%), B (99.5%), and Nb (99.9%), and then RE element, Y (99.9%) were added to the pre-alloy ingot by the arc-melting method. And then, the surface oxide layer on the ingot was removed with a grinder in order to prevent a heterogeneous nucleation.

The thermal stability and phase transition behavior of alloys were observed by a differential scanning calorimeter (DSC) at a heating rate of 0.67 K/s. The supercooled liquid temperature region, which is defined as a temperature spun between the glass transition temperature (T_g) and the onset temperature of crystallization (T_x), $\Delta T_x = T_x - T_g$ was also calculated. In addition, the melting temperature (T_m) and liquidus temperature (T_l) were measured at a cooling rate of 0.17 K/s after complete melting.

*1Corresponding author, E-mail: smlee@imr.tohoku.ac.jp

*2Graduate Student, Tohoku University

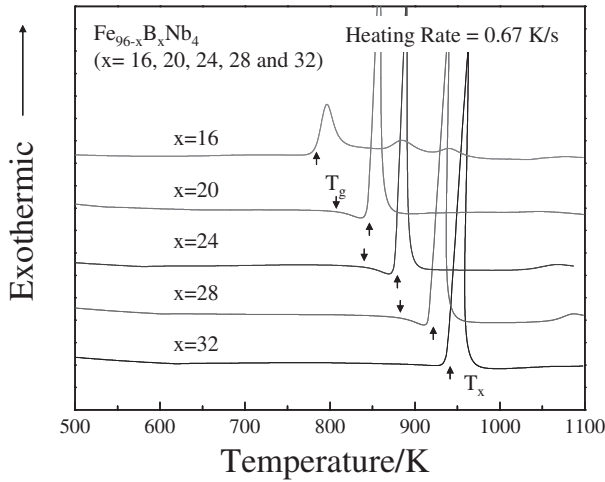


Fig. 1 DSC traces obtained from $\text{Fe}_{96-x}\text{B}_x\text{Nb}_4$ ($x = 16, 20, 24, 28$ and 32) marginal metallic glasses at a heating rate of 0.67 K/s .

The glassy specimens were annealed at different temperatures depending on their T_g and T_x at a heating rate of 0.67 K/s for various annealing periods to investigate their phase transition and crystallization behaviors. The glassy and crystalline phases were confirmed by a X-ray diffractometer (XRD, Rigaku, RAD-B) with $\text{Cu-K}\alpha$ radiation from 20 to 80 degree of 2θ . Nanocrystallization and other phase transition behaviors were observed by using a transmission electron microscope (TEM, JEOL).

Magnetic properties were measured with a vibrating sample magnetometer (VSM, Digital Measurement Systems, VSM-5) for saturation magnetization, B-H loop Tracer for coercivity, respectively. A glassy ring and an amorphous ribbon of $(\text{Fe}_{0.72}\text{B}_{0.24}\text{Nb}_{0.04})_{95.5}\text{Y}_{4.5}$ were used for coercivity measurement for comparison.

3. Results and Discussions

3.1 Glass forming ability of $(\text{Fe}_{0.72}\text{B}_{0.24}\text{Nb}_{0.04})_{100-x}\text{Y}_x$ alloy system

$\text{Fe}_{96-x}\text{B}_x\text{Nb}_4$ ($x = 16, 20, 24, 28$ and 32) compositions were studied for searching the best pre-alloy. The glass transition phenomenon was observed at $x = 20, 24$ and 28 , and the largest value of ΔT_x ($= 39 \text{ K}$) was obtained at $x = 24$ ($\text{Fe}_{72}\text{B}_{24}\text{Nb}_4$) as shown in Fig. 1. The ternary Fe-B-Nb system has been already studied by Imafuku *et al.*¹²⁾ They,

however, investigated the crystallization behavior of $\text{Fe}_{90-x}\text{B}_x\text{Nb}_{10}$ ($x = 10, 20$ and 30) glassy ribbons and discussed the relationship between the stability of supercooled liquid state and the phases formed upon crystallization from the structural point of view. In this study, Nb content is limited to 4 at\% , as considering of the cost and magnetic properties. Furthermore, the high GFA and good magnetic properties are reported in the recent Fe-based BMGs of 4 at\% of Nb bearing compositions. Therefore, $\text{Fe}_{72}\text{B}_{24}\text{Nb}_4$ was selected as a base alloy in this study.

According to the empirical rules suggested by Inoue (Tohoku Univ., Japan),¹³⁾ Y is good candidate for improving GFA of the base alloy since the atomic size difference is 12% or more with Fe, B and Nb. In addition, the heats of mixing among Y and the constituent elements become also large negative values, except for Nb-Y. From thermal properties T_g , T_x , T_m and T_1 , ΔT_x , the reduced glass transition temperature $T_{rg} = T_g/T_1$ and $\gamma = T_x/(T_g + T_1)$, were calculated for estimating GFA of the alloys in Table 1. As increasing Y addition in $(\text{Fe}_{0.72}\text{B}_{0.24}\text{Nb}_{0.04})_{100-x}\text{Y}_x$ alloy system, T_g , T_x and ΔT_x became larger and the value of ΔT_x at 6 at\% Y addition mounts up to 125 K which is considered to be the largest supercooled liquid region among the Fe-based amorphous or glassy alloys developed up to date. But T_{rg} and γ were the highest at 4.5 at\% Y addition since the factors of T_{rg} and γ are relying on the T_1 . The critical glass forming size was enhanced from 0.02 mm in thickness for the base alloy ribbon up to 7 mm in diameter for the 4.5 at\% Y added alloy. Both T_{rg} ($= 0.645$) and γ ($= 0.442$) are the highest at $x = 4.5 \text{ at\%}$. Therefore, these parameters are found to catch the trend of GFA exactly in this alloy system.

3.2 Characteristic exothermic reaction within the supercooled liquid region in $(\text{Fe}_{0.72}\text{B}_{0.24}\text{Nb}_{0.04})_{100-x}\text{Y}_x$ alloy system

The mixing enthalpy of Nb-Y is $+30 \text{ kJ/mol}$. It means that these elements have a tendency to separate each other during the solidification process.^{14–18)} Even though $(\text{Fe}_{0.72}\text{B}_{0.24}\text{Nb}_{0.04})_{100-x}\text{Y}_x$ ($x = 0 \sim 10$) alloys have the large positive mixing enthalpy between Nb-Y, they could be frozen into a meta-stable homogeneous glassy phase due to the high cooling rate. As shown in Fig. 2, it is worthy of pointing out that an exothermic reaction is found within the ΔT_x of the alloys with $\geq 3.5 \text{ at\%}$ Y element.

Figure 2 shows DSC traces obtained from the as-quenched $\text{Fe}_{72}\text{B}_{24}\text{Nb}_4$ glassy ribbon, as-cast $(\text{Fe}_{0.72}\text{B}_{0.24}\text{Nb}_{0.04})_{95.5}\text{Y}_{4.5}$

Table 1 Thermal properties and maximum glass forming diameter of $(\text{Fe}_{0.72}\text{B}_{0.24}\text{Nb}_{0.04})_{100-x}\text{Y}_x$ ($x = 0, 2, 3, 4, 4.5, 5$ and 6) metallic glasses, where T_g : glass transition temperature, T_x : crystallization temperature, ΔT_x : temperature spun of the supercooled liquid state ($= T_x - T_g$), T_m : melting temperature, T_1 : liquidus temperature, reduced glass transition temperature ($= T_g/T_1$), parameter for the glass forming ability ($= T_x/(T_g + T_1)$) and D_{max} : the maximum glass forming parameter by a copper mold casting technique.

Composition	T_g (K)	T_x (K)	ΔT_x (K)	T_m (K)	T_1 (K)	T_{rg}	γ	D_{max} (mm)
$\text{Fe}_{72}\text{B}_{24}\text{Nb}_4$ (base alloy)	837	876	39	1359	1497	0.559	0.375	0.02 (ribbon)
$(\text{Fe}_{0.72}\text{B}_{0.24}\text{Nb}_{0.04})_{98}\text{Y}_2$	855	918	63	1325	1473	0.580	0.394	2.0
$(\text{Fe}_{0.72}\text{B}_{0.24}\text{Nb}_{0.04})_{97}\text{Y}_3$	860	942	82	1326	1430	0.601	0.411	4.0
$(\text{Fe}_{0.72}\text{B}_{0.24}\text{Nb}_{0.04})_{96}\text{Y}_4$	861	959	98	1326	1349	0.638	0.434	6.0
$(\text{Fe}_{0.72}\text{B}_{0.24}\text{Nb}_{0.04})_{95.5}\text{Y}_{4.5}$	871	982	111	1326	1349	0.645	0.442	7.0
$(\text{Fe}_{0.72}\text{B}_{0.24}\text{Nb}_{0.04})_{95}\text{Y}_5$	870	990	120	1324	1445	0.602	0.427	6.0
$(\text{Fe}_{0.72}\text{B}_{0.24}\text{Nb}_{0.04})_{94}\text{Y}_6$	883	1008	125	1330	1431	0.617	0.436	5.0

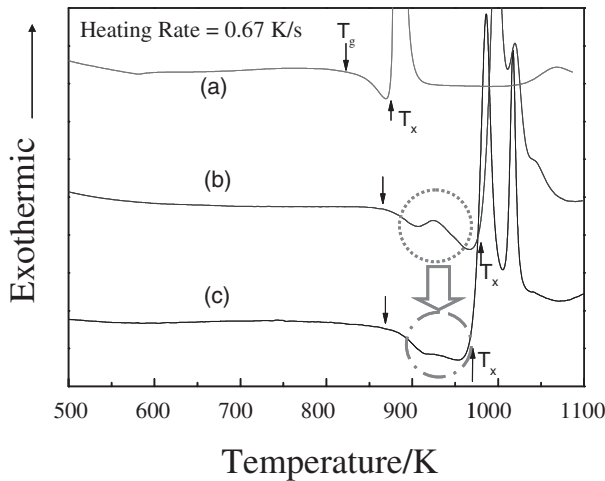


Fig. 2 DSC traces obtained from (a) the as-quenched $\text{Fe}_{72}\text{B}_{24}\text{Nb}_4$ glassy ribbon, (b) as-cast $(\text{Fe}_{0.72}\text{B}_{0.24}\text{Nb}_{0.04})_{95.5}\text{Y}_{4.5}$ BMG (3.0 mm in diameter), and (c) the specimen preliminary annealed up to 928 K. The characteristic exothermic reaction observed in (b) was disappeared by the preliminary heating up to 928 K as shown in (c).

BMG (3.0 mm in diameter), and $(\text{Fe}_{0.72}\text{B}_{0.24}\text{Nb}_{0.04})_{95.5}\text{Y}_{4.5}$ BMG which is once heated up to 928 K to induce the phase transformation. In order to show the effect of Y addition, DSC curve of the ternary $\text{Fe}_{72}\text{B}_{24}\text{Nb}_4$ was also shown in Fig. 2. The exothermic peak at around 928 K of the as-cast $(\text{Fe}_{0.72}\text{B}_{0.24}\text{Nb}_{0.04})_{95.5}\text{Y}_{4.5}$ BMG is so unique that there have been no reports on this phenomenon. The exothermic peak was apparently observed on DSC trace of the alloys with > 3.5 at% Y elements. If a glass transforms to a more stable phase with a lower free energy level like crystal, the surplus energy could be released from the internal to external systems. From this point of view, it can be expected that the present exothermic reaction results from crystallization, phase separation or chemical short-range ordering. To investigate the exothermic transformation on the DSC

traces, the specimen was heated up to 928 K, *i.e.* the top of exothermic peak at a heating rate of 0.67 K/s by DSC, then cooled down to the room temperature. Resulted from this heat treatment, the exothermic peak was clearly disappeared without shifting T_g and T_x , on the DSC trace (c) of the annealed sample in Fig. 2. TEM observation on the $(\text{Fe}_{0.72}\text{B}_{0.24}\text{Nb}_{0.04})_{95.5}\text{Y}_{4.5}$ BMGs annealed at 922 K ($= T_g + 51$ K) for 30 s was carried out, and the results are shown in Fig. 3 as well as that of the as-cast state for comparison. No apparent evidence for the phase transformation was observed in the bright field images, diffraction patterns and HRTEM of both the as-cast and annealed specimens. This indicates that (nano-)crystallization could be excluded from the causes of the present exothermic reaction. Thus the phase separation or chemical short-range ordering is remained as a candidate to explain this phenomenon. In this case, the apparent exothermic phenomenon was observed in DSC curves and the most considerable origin of the phenomenon is chemical short-range ordering. The phase separation is also expected to occur due to the positive enthalpy between Nb and Y, but the contents of both Nb (4 at%) and Y (4.5 at%) are too small to bring about any phase separations. Furthermore, there did not appear any evidences of phase separation even though HRTEM observations as seen in Fig. 3.

3.3 Thermal stability and nanocrystallization of $(\text{Fe}_{0.72}\text{B}_{0.24}\text{Nb}_{0.04})_{95.5}\text{Y}_{4.5}$ BMG

$(\text{Fe}_{0.72}\text{B}_{0.24}\text{Nb}_{0.04})_{95.5}\text{Y}_{4.5}$ glassy ribbon was annealed at T_g ($= 871$ K) for 5.4 ks and 21.6 ks to investigate thermal stability of the alloy. There are no crystallization peaks observed in the XRD patterns for these samples as shown in Fig. 4(a) although T_x (thus ΔT_x) in the DSC curves changed with the annealing time, on the other hand T_g kept a constant value as shown in Fig. 4(b). It is considered to be the first report on the excellent thermal stability at T_g , that thermal stability of over than 21.6 ks at T_g , especially in Fe-/Co-

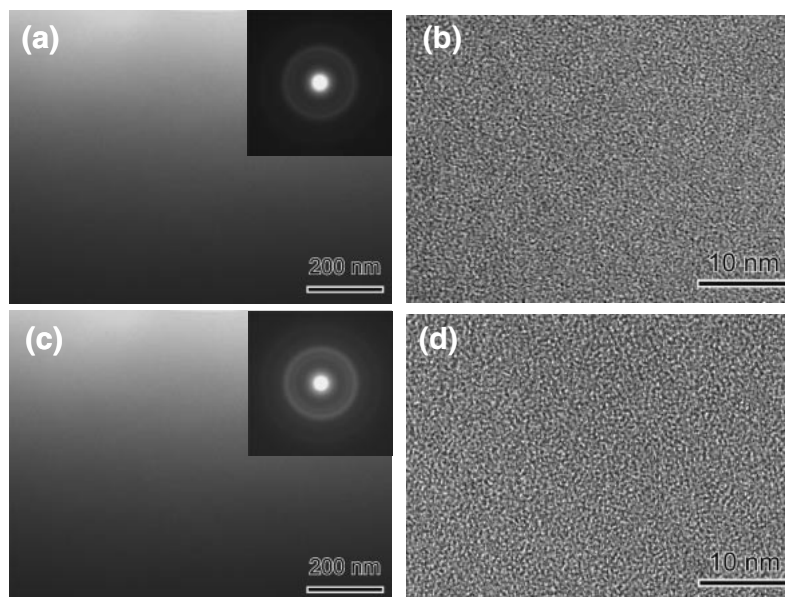


Fig. 3 TEM micrographs, the corresponding selected area diffraction (SAD) patterns and HRTEM images of as-quenched and annealed (at 922 K for 30 s) of $(\text{Fe}_{0.72}\text{B}_{0.24}\text{Nb}_{0.04})_{95.5}\text{Y}_{4.5}$ BMGs ((a) and (b) are of the as-quenched, and (c) and (d) are of the as-annealed samples).

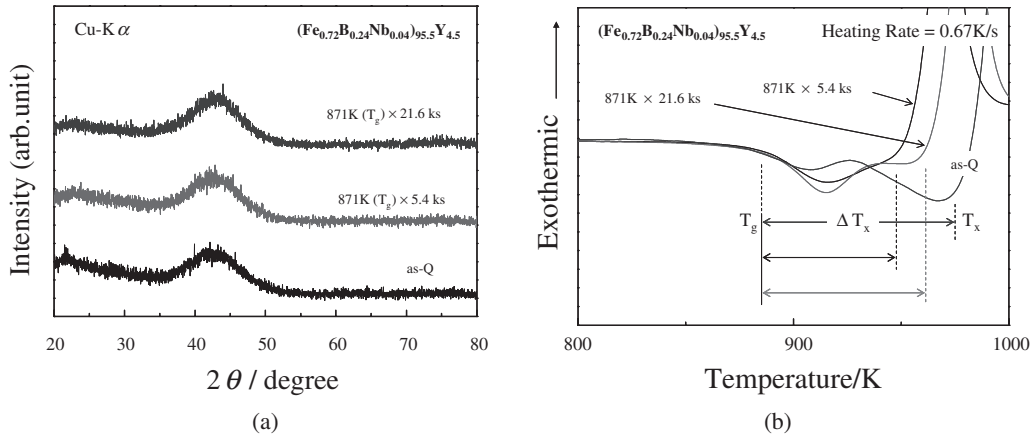


Fig. 4 (a) XRD and (b) DSC traces obtained from $(\text{Fe}_{0.72}\text{B}_{0.24}\text{Nb}_{0.04})_{95.5}\text{Y}_{4.5}$ glassy ribbon at as-quenched and annealed ($@ 871 \text{ K} (= T_g)$) for 5.4 ks and 21.6 ks states.

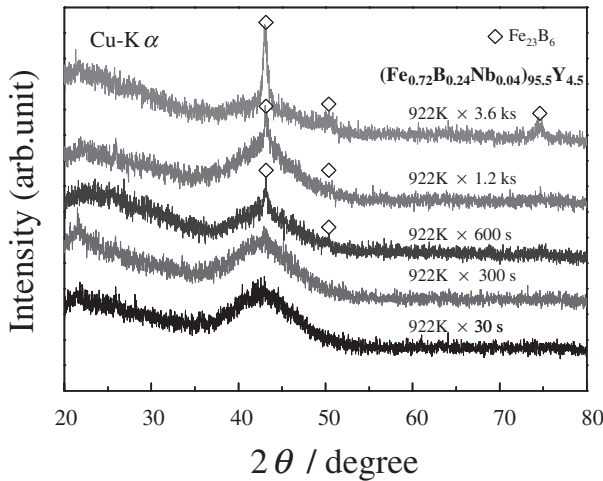


Fig. 5 XRD patterns obtained from $(\text{Fe}_{0.72}\text{B}_{0.24}\text{Nb}_{0.04})_{95.5}\text{Y}_{4.5}$ glassy ribbon annealed at $922 \text{ K} (= T_g + 51 \text{ K})$ with various annealing time as for 30 s, 300 s, 600 s, 1.2 ks and 3.6 ks. The primary phase of this BMG was found to be Fe_{23}B_6 .

based BMGs. The sustaining of the glassy phase during the annealing for 21.6 ks at T_g is a promising characteristic for perpendicular magnetic memory device technology as soft magnetic underlayer and also ultra-small structural devices, since this Fe-based BMGs can be manufactured delicately with using the Newtonian viscous flow at around T_g such by die-casting, and micro-/nano-scale imprinting techniques.

$(\text{Fe}_{0.72}\text{B}_{0.24}\text{Nb}_{0.04})_{95.5}\text{Y}_{4.5}$ glassy ribbon was annealed at $922 \text{ K} (= T_g + 51 \text{ K})$ with various annealing time as for 30 s, 300 s, 600 s, 1.2 ks and 3.6 ks to induce devitrification. The XRD patterns of the annealed specimens in Fig. 5 show crystallization behavior of the glassy ribbon. The sharp peaks diffracted from crystalline phase(s) were appeared at around 43 degree from the annealing time of 600 s, 1.2 ks and 3.6 ks. Even after the long time annealing for 3.6 ks, a broad halo pattern was still observed clearly from 35 to 50 degree. This means that glassy and crystalline phases coexist simultaneously after the annealing, and each of the phases has the high thermal stability as mentioned above even in the supercooled liquid region. The crystalline phase was identified to Fe_{23}B_6 , which is observed well in Fe-based

amorphous ribbons and BMGs containing B and Nb elements.¹²⁾ For more detail observation on the phase transition from the glassy to crystalline phases, the glassy ribbons annealed at 922 K for 1.2 ks was observed by TEM. The electron diffraction pattern, dark field (DF) and HRTEM images of the one annealed at 922 K for 1.2 ks were revealed in Figs. 6(a), (b) and (c)–(f), respectively. As shown in Fig. 5, the samples annealed for 1.2 ks at 922 K consist of glassy and nano-crystalline phases. The size of nanocrystal of the samples annealed for 1.2 ks seems about 50 nm from the DF image in Figs. 6(a). The volume fraction of nanocrystalline phase against the glassy matrix can be estimated to be about 5% by calculating the area of nano-crystalline particle in the images. From Figs. 6(c) and (d) a nanocrystalline aggregation of which size is about 50 nm is observed, and is found to consist of 10 nm size nanocrystalline particles. As shown in Figs. 6(e) and (f) the nanocrystalline particles are showing the ordered configuration, but the interfaces between nanocrystalline phase and glassy matrix are not faceted. The lattice parameter of the nanocrystalline phase is deduced to be about 1 nm, thus this phase is identified to be the Fe_{23}B_6 metastable phase with using the XRD results in Fig. 5. This metastable phase has been often observed in Fe-based bulk glass formers. In the supercooled liquid of these alloys, Fe_{23}B_6 type clusters are considered to be formed and to suppress the atomic diffusion required for formation of the stable crystalline phase, *i.e.* $\alpha\text{-Fe}$. This may help the glass formation in these alloys.

3.4 Soft magnetic properties of $(\text{Fe}_{0.72}\text{B}_{0.24}\text{Nb}_{0.04})_{95.5}\text{Y}_{4.5}$ BMG and their improvement by heat treatment

Figure 7 shows outer morphology and surface appearance of a cast $(\text{Fe}_{0.72}\text{B}_{0.24}\text{Nb}_{0.04})_{95.5}\text{Y}_{4.5}$ rectangular glassy rod with a length of 12 mm, a height of 2 mm and width 2 mm. Saturation magnetization was measured by VSM with using the cast rectangular glassy rod owing to reduce errors from fluctuation of density. In the case of amorphous ribbons, it is so difficult to measure density correctly due to small weight of sample. On the other hands, bulk sample enables us to achieve relatively correct value of density. Density was calculated by Archimedes method with using a tetrabromothane liquid. There were not appeared any differences of

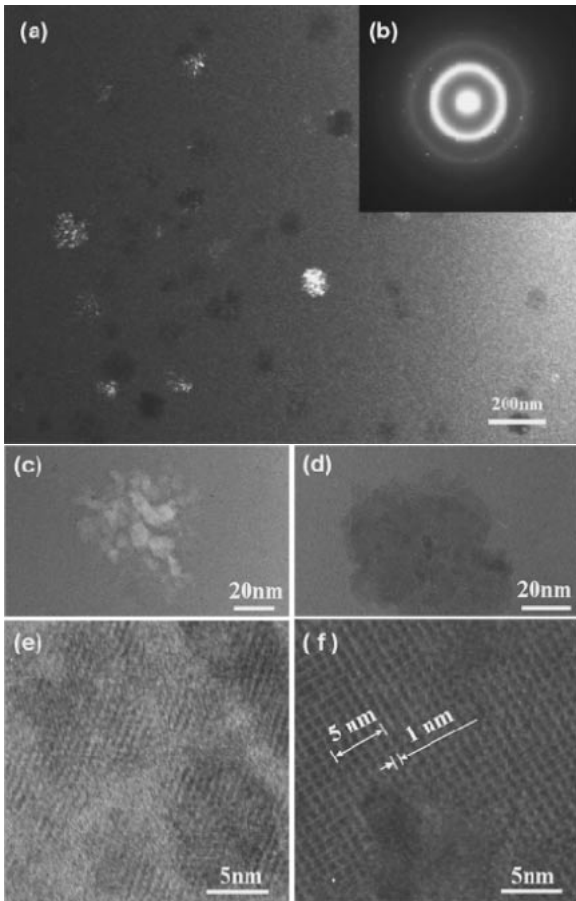


Fig. 6 (a) Dark Field (DF) image, (b) selected diffraction pattern and (c–f) HRTEM images obtained from the $(\text{Fe}_{0.72}\text{B}_{0.24}\text{Nb}_{0.04})_{95.5}\text{Y}_{4.5}$ melt spun ribbon annealed for 1.2 ks at 922 K ($= T_g + 51$ K).

density between as-cast and annealed samples in this study.

As seen in Fig. 8, magnetization curve shows that the annealed rectangular glassy rod has a saturation magnetization, J_s of 0.8 T, which is approximately as same as that for as-cast one. The reason why the saturation magnetization is not changed with thermal treatment is caused by the constant density before/after annealing. The saturation magnetization, J_s of 0.8 T is lower than that for conventional Fe-based amorphous alloys.^{19–21} Compared to the references of Fe-based amorphous alloys including Nb or Y as shown in Table 2, J_s of the composition is lower than that of Fe-based alloys including Nb or Y. A cast ring with a thickness

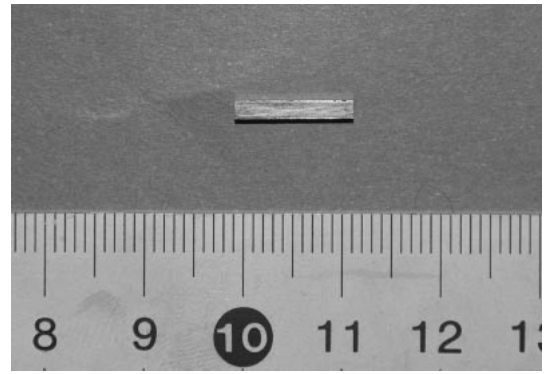


Fig. 7 Outer morphology and surface appearance of a cast rectangular $(\text{Fe}_{0.72}\text{B}_{0.24}\text{Nb}_{0.04})_{95.5}\text{Y}_{4.5}$ glassy alloy rod with a length of 12 mm, a height of 2 mm and width 2 mm.

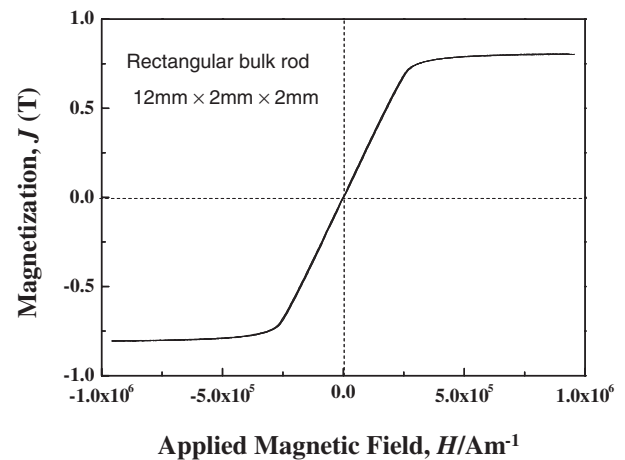


Fig. 8 Magnetization curve of a cast rectangular $(\text{Fe}_{0.72}\text{B}_{0.24}\text{Nb}_{0.04})_{95.5}\text{Y}_{4.5}$ glassy alloy rod with a length of 12 mm, a height of 2 mm and width 2 mm.

0.5 mm, an outer diameter of 10 mm and an inner diameter of 6 mm was prepared to investigate coercivity, H_c as shown in Fig. 9. The coercivities were measured by B-H analyzer with using both an amorphous ribbon and a cast $(\text{Fe}_{0.72}\text{B}_{0.24}\text{Nb}_{0.04})_{95.5}\text{Y}_{4.5}$ glassy ring in order to investigate the effect of shape on coercivity. Figure 10 shows the B-H hysteresis curves of a cast $(\text{Fe}_{0.72}\text{B}_{0.24}\text{Nb}_{0.04})_{95.5}\text{Y}_{4.5}$ glassy ring and an amorphous ribbon after annealing at 821 K ($= T_g - 50$ K) for 300 s. The annealed cast ring has H_c of 0.8 A/m, which is descended from 1.0 A/m for that of as-cast

Table 2 A comparison of saturation magnetization (J_s) and coercivity (H_c) for various Fe-based amorphous alloys.

Composition		J_s (T)	H_c (A/m)	References
$(\text{Fe}_{0.75}\text{B}_{0.15}\text{Si}_{0.10})_{99}\text{Nb}_1$	—	1.50	3.7	19)
$(\text{Fe}_{0.75}\text{B}_{0.15}\text{Si}_{0.10})_{96}\text{Nb}_4$	—	1.47	2.9	19)
$\text{Y}_4\text{Fe}_{76}\text{B}_{20}$	—	1.56	—	20)
$\text{Y}_6\text{Fe}_{72}\text{B}_{22}$	—	1.47	4.0	20)
$\text{Fe}_{80}\text{B}_{11}\text{Si}_9$	—	1.59	—	21)
$(\text{Fe}_{0.72}\text{B}_{0.24}\text{Nb}_{0.04})_{95.5}\text{Y}_{4.5}$	Ribbon (as-quenched)	—	20	This study
$(\text{Fe}_{0.72}\text{B}_{0.24}\text{Nb}_{0.04})_{95.5}\text{Y}_{4.5}$	Ribbon (annealed)	—	0.2–0.5	This study
$(\text{Fe}_{0.72}\text{B}_{0.24}\text{Nb}_{0.04})_{95.5}\text{Y}_{4.5}$	Bulk (as-quenched)	0.8	1.0	This study
$(\text{Fe}_{0.72}\text{B}_{0.24}\text{Nb}_{0.04})_{95.5}\text{Y}_{4.5}$	Bulk (annealed)	0.8	0.8	This study

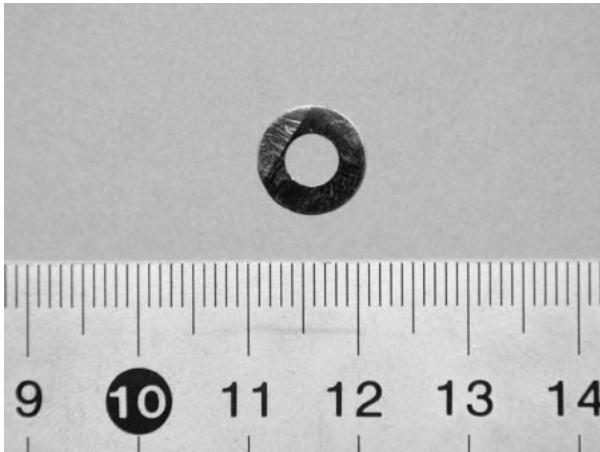


Fig. 9 Outer morphology and surface appearance of a cast $(\text{Fe}_{0.72}\text{B}_{0.24}\text{Nb}_{0.04})_{95.5}\text{Y}_{4.5}$ glassy alloy ring with a thickness 0.5 mm, an outer diameter of 10 mm and an inner diameter of 6 mm.

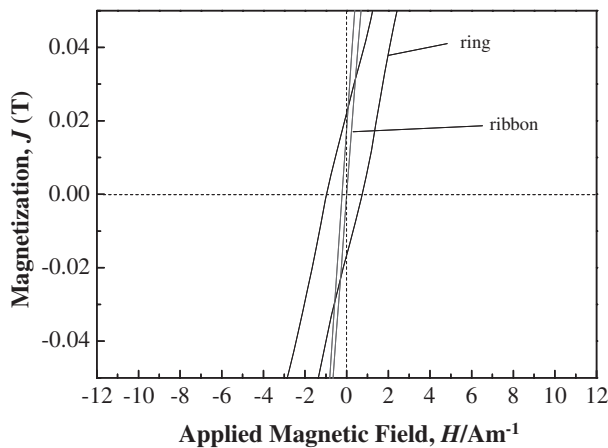


Fig. 10 B-H hysteresis curves of a cast $(\text{Fe}_{0.72}\text{B}_{0.24}\text{Nb}_{0.04})_{95.5}\text{Y}_{4.5}$ glassy ring and an amorphous ribbon after annealing at 821 K ($= T_g - 50$ K) for 300 s.

one. The annealed amorphous ribbon has H_c of 0.2–0.5 A/m, which also decreased from 20–30 A/m for that of as-quenched one.

The H_c of 0.2–0.5 A/m after annealing is the lowest value among the Fe-based soft magnetisms which have been developed up to date. The origin of the novel H_c of 0.2–0.5 A/m may be caused by high structural homogeneity in the Y-added alloy closely related to the high GFA and oxygen scavenging effect through the formation of yttrium oxide during arc-melting and copper mold casting/melt-spinning processes.²²⁾ Y atoms have a stronger affinity ($\text{Y}_2\text{O}_3 = -1904$ KJ/mol) to the oxygen atoms than Fe atoms ($\text{Fe}_2\text{O}_3 = -820.5$ KJ/mol),²³⁾ Y addition thus can decrease the coercivity by descend of ferromagnetic portion from the alloy.

The difference of H_c between 0.8 A/m of a glassy ring and 0.2–0.5 A/m of an amorphous ribbon can be explained by the defects in the bulk glassy ring sample. The possibility of defects such as contamination and vacancy might be higher in bulk glassy samples than in amorphous ribbons. In this study, a large of fluctuation on density was discovered in the

bulk glassy samples which can have some defects due to the wrong casting condition. In the case of other amorphous ribbons, it has been reported that densities may increase by appropriate thermal treatments due to decrease of vacancy in the ribbons.²⁴⁾ On the other hands, vacancy in a bulk sample is expected to remain in spite of thermal annealing. Therefore, the best casting condition should be acquired to solve the original defects problem during casting process for applications of the Fe-based BMGs.

4. Conclusion

The effects of Y addition on the glass forming ability (GFA) of a Fe-B-Nb marginal glass former, and annealing effects on glassy/supercooled liquid phases and soft magnetic properties in the multicomponent Fe-B-Nb-Y alloy system were investigated. The results can be summarized as follows.

- (1) In a Fe-B-Nb ternary marginal glass forming system, a $\text{Fe}_{72}\text{B}_{24}\text{Nb}_4$ (at%) alloy was found to have the largest supercooled liquid temperature region (ΔT_x) of 39 K at a heating rate of 0.67 K/s and critical glass forming size of 0.02 mm.
- (2) Y addition was confirmed to improve GFA of the $\text{Fe}_{72}\text{B}_{24}\text{Nb}_4$ alloy. The maximum critical glass forming diameter in $(\text{Fe}_{0.72}\text{B}_{0.24}\text{Nb}_{0.04})_{100-x}\text{Y}_x$ ($x = 0 \sim 6$) system was 7 mm (350 times larger than the $\text{Fe}_{72}\text{B}_{24}\text{Nb}_4$ base alloy) of an $(\text{Fe}_{0.72}\text{B}_{0.24}\text{Nb}_{0.04})_{95.5}\text{Y}_{4.5}$ alloy.
- (3) Characteristic exothermic phase transformation within the supercooled liquid region was observed for the alloys with ≥ 3.5 at% Y element. This is considered to be resulted from a chemical short range ordering associated with the large positive heat of mixing between Nb-Y elements.
- (4) $(\text{Fe}_{0.72}\text{B}_{0.24}\text{Nb}_{0.04})_{95.5}\text{Y}_{4.5}$ alloy was found to maintain a single glassy phase even after a heat treatment at T_g ($= 871$ K) for 21.6 ks ($= 6$ hours). This indicates that this bulk metallic glass has distinct higher-thermal stability with compared to other Fe-/Co- based bulk metallic glasses developed up to date.
- (5) Saturation magnetization and coercivity of the as-cast $(\text{Fe}_{0.72}\text{B}_{0.24}\text{Nb}_{0.04})_{95.5}\text{Y}_{4.5}$ glassy ring were found to be 0.8 T and 0.8 A/m after annealing, respectively. In addition, lower coercivity of 0.2–0.5 A/m was achieved by the appropriate heat treatment in the amorphous ribbon sample. The origin of excellent soft magnetism is considered to be caused by homogeneity and oxygen scavenging effect.

Acknowledgement

This work was supported by a Grant-in-Aid for Scientific Research on Priority Areas, “Materials Science of Bulk Metallic Glasses”, from the Ministry of Education, Science, Sports and Culture of Japan.

REFERENCES

- 1) A. Inoue, T. Zhang and N. Nishiyama: Mater. Trans., JIM **34** (1993) 1234.

- 2) A. Inoue, T. Zhang and N. Nishiyama: *Mater. Trans., JIM* **34** (1991) 1005.
- 3) A. Peker and W. L. Johnson: *Appl. Phys. Lett.* **63** (1993) 2342.
- 4) D. H. Kim, J. M. Park, D. H. Kim and W. T. Kim: *J. Mater. Res.* **22** (2007) 471.
- 5) P. Pawlik and H. A. Davies: *Scripta Mater.* **49** (2003) 755.
- 6) Y. Long, W. Zhang, X. Wang and A. Inoue: *J. Appl. Phys.* **91** (2002) 5227.
- 7) K. Amiya, A. Urata, N. Nishiyama and A. Inoue: *Mater. Trans., JIM* **45** (2004) 1214.
- 8) D. S. Song, J. H. Kim, E. Fluery, W. T. Kim and D. H. Kim: *J. Alloys Compd.* **389** (2005) 159.
- 9) V. Ponnambalam, S. J. Poon and G. J. Shiflet: *J. Mater. Res.* **19** (2004) 1320.
- 10) J. Shen, Q. J. Chen, J. F. Sun, H. B. Fan and G. Wang: *Appl. Phys. Lett.* **86** (2005) 151907.
- 11) Z. Han *et al.*: *Intermetallics* **15** (2007) 1447.
- 12) M. Imafuku, S. Sato, H. Koshihara, E. Matsubara and A. Inoue: *Scripta Mater.* **44** (2001) 2369.
- 13) A. Inoue: *Mater. Trans., JIM* **36** (1995) 866.
- 14) A. Inoue, T. Zhang and T. Masumoto: *Mater. Trans., JIM* **31** (1990) 177.
- 15) A. Inoue, T. Zhang and T. Masumoto: *Mater. Trans., JIM* **30** (1989) 965.
- 16) T. Zhang, A. Inoue, S. Chen and T. Masumoto: *Mater. Trans., JIM* **33** (1992) 143.
- 17) T. B. Massalski, ed.: *Binary alloy phase diagrams* (ASM, Ohio, 1986) p. 2159.
- 18) H. S. Chen: *Rept. Progr. Phys.* **43** (1980) 353.
- 19) A. Inoue and B. Shen: *Mater. Trans., JIM* **43** (2002) 766.
- 20) C.-Y. Lin, H.-Y. Tien and T.-S. Chin: *Appl. Phys. Lett.* **86** (2005) 162501.
- 21) N. DeCristofaro: *MRS Bull.* **23** (1998) 50.
- 22) J. M. Park, J. S. Park, J. H. Na, D. H. Kim and D. H. Kim: *Mater. Sci. Eng., A* **435–436** (2007) 425.
- 23) O. Kubaschewski and C. B. Alcock: *Metallurgical Thermochemistry*, (Pergamon, Oxford, 1979).
- 24) A. Makino *et al.*: *Mater. Trans., JIM* **48** (2007) 3024.